Single ionization of the water molecule by electron impact: Angular distributions at low incident energy

C. Champion,[1] C. Dal Cappello,[1] S. Houamer,[2] and A. Mansouri[2]
[1]*Laboratoire de Physique Moléculaire et des Collisions, Institut de Physique, Université Paul Verlaine-Metz, 1 Boulevard Arago, 57078 Metz Cedex 3, France*
[2]*Département de physique, Faculté des sciences, Université Ferhat Abbas, Sétif, Algeria*
(Received 5 August 2005; revised manuscript received 18 October 2005; published 27 January 2006)

Recent experimental results of Milne-Brownlie *et al.* on the ionization of the water molecule by low-energy electron (250 eV) have been compared to theoretical predictions performed in the distorted-wave first Born model [Phys. Rev. A **69**, 032701 (2004)]. It was found that this theory was unable to predict the very large recoil scattering observed experimentally. In this work, more sophisticated theoretical models are investigated in order to better understand the water ionization process at the multidifferential level and to reproduce the experimental observations.

DOI: 10.1103/PhysRevA.73.012717 PACS number(s): 34.80.Dp

I. INTRODUCTION

Ionization by electron impact is one of the most important challenges in several fields of physics such as plasma physics, diagnostics for fusion in tokamaks, astrophysics, and irradiation of living matter, and has therefore been theoretically and experimentally studied with a great interest for many atomic systems. In this context, the electron-electron coincidence experiments, called $(e,2e)$ experiments, provide a useful description of the kinematics of the collision by giving information about the direction of the scattered and ejected electrons. The quantity measured in this kind of experiment is proportional to the triple differential cross section (TDCS), which represents the angular distribution of the ejected electron for selected incident and scattered electron momenta. A particular aspect of these experiments, called EMS (for electron momentum spectroscopy), refers specifically to intermediate-energy electron impact ionization experiments with a simultaneous detection of the outgoing particles. Thus, by adjusting the experimental parameters, useful information about the target wave function can be found by means of a straightforward relation between the measured differential cross section and the momentum density. A lot of EMS studies already exist in the literature (see, for example, the review given by Coplan *et al.* [1]). On the other hand, dynamical studies of the $(e,2e)$ process have been extensively performed both theoretically and experimentally for atomic targets (see, for example, the review given by Lahmam-Bennani [2]) but remain until today very rare for molecular targets, mainly due to the difficulty in describing the multielectron process and also in finding tractable target wave functions. In fact, the $(e,2e)$ quantum calculations for molecular targets are still an open problem, even in the first Born approximation (FBA), since one needs to calculate generalized oscillator strengths which is a difficult task for molecules. Thus, quantum mechanical ionization studies have been essentially performed for small molecules such as H_2 [3,4], N_2 [3,5–7], N_2O [8], and O_2 [9], in contrast with larger targets for which only semiempirical and semiclassical formulas have been proposed. Such methods formulated in the early 1980s have been discussed by Younger and Märk [10] who described two of them: a first one in which the molecular ionization cross sections are expressed as the sum of the ionization cross sections of the constituent atoms of the molecule, and a second one modified by Khare and Meath [11] to be applied to partial and dissociative ionization cross sections. In general, these theories overestimate the total ionization cross sections and are only in qualitative agreement with the experimental data. More recently, Kim and Rudd [12,13] have developed a "binary-encounter-dipole model" which combines the binary encounter theory of Vriens [14] with the dipole interaction of the Bethe theory [15] for fast incident electrons. The semiempirical calculations present very good agreements with the experimental measurements but remain valid only for single differential and total ionization cross sections.

The description of the ionization process at the multidifferential level needs sophisticated theoretical calculations that do exist for atomic targets but that remain scarce for molecules. The first models were the plane wave impulse approximation (PWIA) and the FBA. In the PWIA, all the electrons (the incident, the scattered, and the ejected ones) are described by a plane wave. In fact, such a model is able to describe experiments at high incident energies and for relatively high ejected energies (of about three times the ionization threshold): a large part of the experiments of Cherid *et al.* [4] (for H_2 ionization) has been described by this model. When the ejected electron energy decreases, one preferentially uses the FBA in which the ejected electron is described by a Coulomb wave or a distorted wave (DWBA), whereas the incident and the scattered electrons are still described by plane waves. For instance, Zurales and Lucchese [16] used a FBA model (for H_2 ionization) in which the ejected electron was described by an orthogonalized Coulomb wave (OCW) or by a distorted wave, which takes into account the interaction between the ejected electron and the residual target. For low scattered energies or when the scattered energy is comparable to the ejected one, one may use the Branner, Briggs, and Klar (BBK) model [17] or the second Born model [18]. In the first one, the final state is de-

scribed by the product of three Coulomb waves, and takes into account the interaction between the scattered electron and the nucleus, the interaction between the ejected electron and the nucleus, and the electron-electron repulsion. This sophisticated model has been applied by Stia *et al.* [19] for H_2 ionization but contains many approximations due to the use of a multicenter initial wave function. In the second Born model, the collision process is considered as a double interaction between the projectile and the target with a scattered electron described by a plane wave and an ejected electron described by a Coulomb wave (or a distorted wave). This latter model needs the introduction of intermediate states of the target and has been applied in the case of the ionization of H_2 by electron impact [18].

The case of the water molecule is even more dramatic since we find in the literature very rare experimental studies. We can cite the extensive work given by Opal *et al.* [20] who provides both double differential cross section (DDCSs) and single differential cross section (SDCSs) for an incident energy of $E_i=500$ eV, an ejected-energy range $E_e=4.13$–205 eV, and ejected angles $\theta_e=30°-180°$. The work of Bolorizadeh and Rudd [21] and that of Oda [22] are dedicated to energetic electrons with an incident energy of $E_i=500$ eV. Concerning the single differential cross sections and the total cross sections (TCSs), the literature is more abundant and several experimental measurements are available for a large range of incident energies [23–34].

However, very recently Milne-Brownlie *et al.* [35] have published experimental TDCS's for electron-impact ionization of the water molecule for an incident energy $E_i=250$ eV, an ejected energy $E_e=10$ eV, and a scattered angle $\theta_s=15°$. The cross section measurements have been performed for the four outer molecular subshells denoted $^1B_1$, $^3A_1$, $^1B_2$, and $^2A_1$ and were found to exhibit a very large recoil scattering unpredicted by the existing theories. In fact, the more recent theoretical study reported by Champion *et al.* [36,37] in the DWBA framework reproduced well the shape of the TDCS's (especially in the binary region) but was unable to predict the recoil structure experimentally observed. Indeed, the binary peak theoretically obtained, with its double-peak structure for the outer valence $^1B_1$ and $^3A_1$ orbitals (due to the *p* character of these orbitals), was in good agreement with experiment but contrary to the experience no recoil peak was found by the theory for the $^1B_1$ and $^2A_1$ orbitals. The authors linked this inability of the theory to reproduce the recoil scattering to the use of plane waves in the incident and outgoing channels and proposed to use distorted waves in all channels as in the calculations performed by Monzani *et al.* for H_2 ionization [38]. In view of this, we present in this work a theoretical approach which consists in improving the theory presented in [37] via more sophisticated models: (i) a first one where the incident electron-neutral target interaction has been introduced, (ii) a second one where the scattered electron-ionized target interaction has been added, and finally (iii) a third one (the BBK or DS3C model) where all the interactions have been taken into account, i.e., the interaction of the ionized target with the projectile electron as well as the ejected electron and the repulsion between the outgoing electrons.

The present paper is organized as follows: In Sec. II the different theoretical models are presented and analyzed by highlighting, in particular, their discrepancies and their similarities, in Sec. III the TDCS's calculated in each model are compared to the experiments, and finally, in Sec. IV a conclusion about the modeling of the ionization of the water molecule is given. Atomic units are used throughout unless otherwise indicated.

II. THEORY

The water molecule ionization process considered in this work can be schematized by

$$e^- + H_2O \rightarrow 2e^- + H_2O^+, \tag{1}$$

and will be regarded as a pure electronic transition since the closure relation over all possible rotational and vibrational states of the residual target can be applied: the relation between the collision time and the characteristic time of rotation and vibration justifies this. Moreover, the exchange effects will be neglected since the scattered electron is faster than the ejected one in all the cases considered here. However, they could eventually be taken into account in the theoretical models developed here.

In the Born approximation, the triple differential cross section is given by

$$\frac{d^3\sigma}{d\Omega_e d\Omega_s dE_e} = \frac{k_e k_s}{k_i}|M|^2, \tag{2}$$

where Ω_s and Ω_e represent the solid angles of detection for the scattered and the ejected electrons, respectively. The momenta $\vec{k}_i$, $\vec{k}_s$, and $\vec{k}_e$ are, respectively, related to the incident, the scattered and the ejected electron, and depend on the corresponding energy through the relation $k_i^2=2E_i$, $k_e^2=2E_e$, and $k_s^2=2E_s$. The matrix element M describes the transition of the system from the initial state Ψ_i to the final state Ψ_f. It is written as

$$M = \frac{1}{2\pi}\langle \Psi_f | V | \Psi_i \rangle, \tag{3}$$

where V represents the interaction between the incident electron and the target and is written as

$$V = -\frac{8}{r_0} - \frac{1}{|\vec{r}_0 - \vec{R}_1|} - \frac{1}{|\vec{r}_0 - \vec{R}_2|} + \sum_{i=l}^{i=10} \frac{1}{|\vec{r}_0 - \vec{r}_i|}, \tag{4}$$

with $R_1=R_2=R_{OH}=1.814$ a.u. while $\vec{r}_i$ is the position of the *i*th bound electron of the target with respect to the oxygen nucleus.

A. The initial state wave function

The initial state which corresponds to an incident electron and the ten bound ones of the target is described by the product of two wave functions: the first one for the incident electron and the second one for the ten bound electrons

$$|\Psi_i\rangle = \left|\phi(\vec{k}_i, \vec{r}_0)\varphi_i(\vec{r}_1, \vec{r}_2, \ldots, \vec{r}_{10})\right\rangle. \tag{5}$$

Whereas the incident electron is described by a plane wave $\phi(\vec{k}_i, \vec{r}_0)$ with its position vector $\vec{r}_0$ (the oxygen nucleus

being the origin), the ten bound electrons are distributed among the five one-center molecular wave functions $\upsilon_j(\vec{r})$ (with j ranging from 1 to 5) corresponding to the orbitals $^1B_1$, $^3A_1$, $^1B_2$, $^2A_1$, and $^1A_1$, respectively. Each of them is expressed by linear combinations of Slater-type functions [39] and is written as

$$\upsilon_j(\vec{r}) = \sum_{k=1}^{N_j} a_{jk} \Phi^{\xi_{jk}}_{n_{jk} l_{jk} m_{jk}}(\vec{r}), \tag{6}$$

where N_j is the number of Slater functions used in the development of the jth molecular orbital and a_{jk} the weight of each real atomic component $\Phi^{\xi_{jk}}_{n_{jk} l_{jk} m_{jk}}(\vec{r})$ (more details can be found in [36,37] and more recently in [40]).

In Eq. (6), $\Phi^{\xi_{jk}}_{n_{jk} l_{jk} m_{jk}}(\vec{r})$ is written as

$$\Phi^{\xi_{jk}}_{n_{jk} l_{jk} m_{jk}}(\vec{r}) = R^{\xi_{jk}}_{n_{jk}}(r) S_{l_{jk} m_{jk}}(\hat{r}), \tag{7}$$

where the radial part $R^{\xi_{jk}}_{n_{jk}}(r)$ is given by

$$R^{\xi_{jk}}_{n_{jk}}(r) = \frac{(2\xi_{jk})^{n_{jk}+1/2}}{\sqrt{(2n_{jk})!}} r^{\,n_{jk}-1} e^{-\xi_{jk} r}, \tag{8}$$

and where $S_{l_{jk} m_{jk}}(\hat{r})$ is the so-called real solid harmonic [41] expressed by

if $m_{\mathrm{jk}} \neq 0$:

$$S_{l_{jk} m_{jk}}(\hat{r}) = \left(\frac{m_{jk}}{2|m_{jk}|}\right)^{1/2} \left\{ Y_{l_{jk}-|m_{jk}|}(\hat{r}) + (-1)^{m_{jk}} \left(\frac{m_{jk}}{|m_{jk}|}\right) Y_{l_{jk}|m_{jk}|}(\hat{r}) \right\}, \tag{9}$$

$$\text{if } m_{\mathrm{jk}} = 0: \quad S_{l_{jk}0}(\hat{r}) = Y_{l_{jk}0}(\hat{r}). \tag{10}$$

Moreover, it is important to note that the molecular wave functions $\upsilon_j(\vec{r})$, initially given by Moccia [39], refer to the calculated equilibrium configurations, i.e., to the geometrical configurations which, among many others considered, give the minimum of the total energy, and agree very well with the experimental data (see [36,37] for a summary).

B. The final state wave function

In this work, four models will be investigated. In each of them, the final state is characterized by the product of two wave functions as

$$|\Psi_f\rangle = |\Psi_{f1}\Psi_{f2}\rangle, \tag{11}$$

where Ψ_{f1} describes the system consisting of the scattered and the ejected electrons while Ψ_{f2} describes the nine bound electrons of the target. Moreover, by using the well-known frozen-core approximation we reduce this ten-electron problem to a one active electron problem. In this case the matrix element can be rewritten as

$$M = \frac{1}{2\pi} \left\langle \Psi_{f1}(\vec{k}_s, \vec{r}_0, \vec{k}_e, \vec{r}_1) \left| \frac{1}{r_{01}} - \frac{1}{r_0} \right| \phi(\vec{k}_i, \vec{r}_0) \upsilon_j(\vec{r}_1) \right\rangle. \tag{12}$$

In a first model developed in the first Born approximation, the incident and the scattered electrons are described by plane waves, whereas the ejected one is described by a Coulomb wave (FBA-CW) [36] or a DWBA [37]. Thus, Ψ_{f1} can be written as

$$\left|\Psi_{f1}(\vec{k}_s, \vec{r}_0, \vec{k}_e, \vec{r}_1)\right\rangle = \left|\exp(i\vec{k}_s \cdot \vec{r}_0) \varphi_c(\vec{k}_e, \vec{r}_1)\right\rangle, \tag{13}$$

with

$$\varphi_c(\vec{k}_e, \vec{r}) = \sum_{l=0}^{\infty} \sum_{m=-l}^{m=+l} 4\pi (i)^l \exp[-i(\sigma_l + \delta_l)] \times \frac{F_l(k_e; r)}{k_e r} Y_{lm}(\hat{k}_e) \mathrm{Y}_{lm}(\hat{r}), \tag{14}$$

where σ_l and δ_l represent the Coulomb phase shift and the short-range phase shift associated with the distortion potential $W(r)$, respectively. The radial regular function $F_l(k_e; r)$ is then solution of the differential equation

$$\left[\frac{1}{2}\frac{d^2}{dr^2} + E_e - \frac{l(l+1)}{2r^2} - W(r)\right] F_l(k_e; r) = 0, \tag{15}$$

and exhibits an asymptotic behavior given by

$$F_l(k_e; r) \sim \sin\left(k_e r - l\frac{\pi}{2} + \frac{1}{k_e}\ln(2\, k_e \mathrm{r}) + \sigma_l + \delta_l\right). \tag{16}$$

Let us note that when $\delta_l = 0$, $\varphi_c(\vec{k}_e, \vec{r})$ becomes a Coulomb wave which can be rewritten as

$$\varphi_c(\vec{k}_e, \vec{r}) = \frac{\exp(iZ_e/k_e)}{(2\pi)^{3/2}} {}_1F_1\left[-iZ_e/k_e, 1, -i(\vec{k}_e \,.\, \vec{r} + k_e r)\right] \times \exp\left(\frac{\pi Z_e}{2k_e}\right) \Gamma(1 + iZ_e/k_e), \tag{17}$$

and can be calculated with analytical formulas (Dal Cappello *et al.* [42], Brothers and Bonham [43]). Here, the well-known Sommerfeld parameter, defined as the ratio between the product of the charges of the particles and their relative momentum, is equal to Z_e/k_e where Z_e corresponds to the effective ionic charge (Brothers and Bonham [43]). In this model, denoted in the following as 1CW model, Z_e will be taken to be equal to 1.

In a second model, the scattered and ejected electrons are both described by a Coulomb wave (2CW) [44]. Similarly as the previous model, the charges Z_e and Z_s seen by the escaping electrons will be defined as the effective ionic charges [44] and will be taken to be equal to 1. In this model

$$\Psi_{f1}(\vec{k}_s, \vec{r}_0, \vec{k}_e, \vec{r}_1) = \frac{\exp(iZ_s/k_s)}{(2\pi)^{3/2}} {}_1F_1\left[-iZ_s/k_s, 1, -i(\vec{k}_s \,.\, \vec{r}_0 + k_s r_0)\right] \times \exp\left(\frac{\pi Z_s}{2k_s}\right) \Gamma(1 + iZ_s/k_s) \times \frac{\exp(iZ_e/k_e)}{(2\pi)^{3/2}} {}_1F_1\left[-iZ_e/k_e, 1, -i(\vec{k}_e \cdot \vec{r}_1 + k_e r_1)\right]$$

$$\times \exp\left(\frac{\pi Z_e}{2k_e}\right)\Gamma(1+iZ_e/k_e). \tag{18}$$

In a third approach, we have used one of the most sophisticated models, called the BBK model [17] which was initially developed for ionization of hydrogen atoms by electron and positron impact. The main characteristic of this model consists in exhibiting a correct asymptotical Coulomb three-body wave function for the ejected and scattered electrons in the residual ion field. This important property is at the origin of the large disagreement observed between the theoretical work on the ionization of H_2 by electron impact of Monzani *et al.* [38] based on the distorted-wave model within the Born-Oppenheimer approximation (DWBO) (which neglects the multichannel effects as well as the post-collisional correlation between the two outgoing electrons) and the theoretical work of Stia *et al.* [19] based on the BBK model. For this reason, we will consider this model for the present water ionization process.

It is worth noting that the results obtained in the BBK model were not in agreement with experiment in the case of low-energy measurements of H and He ionization [45–47]. Thus, Berakdar and Briggs have proposed to improve this model by introducing effective Sommerfeld parameters in the two-body factors in the BBK wave function [48]. Indeed, since the Sommerfeld parameter corresponds to a measure of the strength of the Coulomb interaction between two particles, this latter is obviously affected by the presence of the third particle. Therefore, the new (effective) Sommerfeld parameters introduced here should be functions of the three relative momenta [see Eqs. (21), (22), and (23)]. This new model, called the DS3C model (for dynamic screening of the three two-body Coulomb interactions), has been first applied to symmetric geometries [48]. However, since the experiments and investigations of Milne-Brownlie *et al.* have been performed in asymmetric geometries, we have preferred to use the extended DS3C model proposed by Zhang [49] for asymmetric situations. Finally, let us note that the results given by this approach in the case of He ionization by electron impact are comparable to those provided by the powerful convergent close-coupling (CCC) calculations [50,51].

In both cases (BBK and DS3C models) we have the well-known asymptotically correct Coulomb three-body wave function for the ejected and scattered electrons in the field of the residual ion [17]

$$\begin{aligned}\Psi_{f1}(\vec{k}_s,\vec{r}_0,\vec{k}_e,\vec{r}_1) = {} & \frac{\exp(iZ_s/k_s)}{(2\pi)^{3/2}}\,{}_1F_1\left[-iZ_s/k_s,1,-i(\vec{k}_s\cdot\vec{r}_0 + k_s r_0)\right]\exp\left(\frac{\pi Z_s}{2k_s}\right)\Gamma(1+iZ_s/k_s) \\ & \times \frac{\exp(iZ_e/k_e)}{(2\pi)^{3/2}}\,{}_1F_1\left[-iZ_e/k_e,1,-i(\vec{k}_e\cdot\vec{r}_1 + k_e r_1)\right]\exp\left(\frac{\pi Z_e}{2k_e}\right)\Gamma(1+iZ_e/k_e) \\ & \times {}_1F_1\left[iZ_{se}/k_{se},1,-i(\vec{k}_{se}\cdot\vec{r}_{01} + k_{se}r_{01})\right]\exp\left(\frac{-\pi Z_{se}}{4k_{se}}\right)\Gamma(1-iZ_{se}/2k_{se}),\end{aligned} \tag{19}$$

where k_{se} is the relative momentum

$$k_{se} = \tfrac{1}{2}\left|\vec{k}_s - \vec{k}_e\right|, \tag{20}$$

with $Z_s = Z_e = Z_{se} = 1$ in the BBK model whereas in the DS3C model they are given by, respectively [49]

$$Z_s = 1 - \frac{2k_{se}k_s^2}{(k_s+k_e)^3}\left(\frac{3+\cos^2(4\varepsilon(k_e))}{4}\right)^2, \tag{21}$$

$$Z_e = 1 - \frac{2k_{se}k_e^2}{(k_s+k_e)^3}\left(\frac{3+\cos^2(4\varepsilon(k_s))}{4}\right)^2, \tag{22}$$

and

$$\begin{aligned}Z_{se} = {} & 1 - \frac{2k_{se}k_s^2}{(k_s+k_e)^3}\left(\frac{3+\cos^2(4\varepsilon(k_e))}{4}\right)^2\frac{2k_{se}}{k_s} \\ & - \frac{2k_{se}k_e^2}{(k_s+k_e)^3}\left(\frac{3+\cos^2(4\varepsilon(k_s))}{4}\right)^2\frac{2k_{se}}{k_e},\end{aligned} \tag{23}$$

with

$$\varepsilon(k_e) = \arccos\left(\frac{k_e}{\sqrt{k_s^2+k_e^2}}\right)$$

$$\varepsilon(k_s) = \arccos\left(\frac{k_s}{\sqrt{k_s^2+k_e^2}}\right). \tag{24}$$

III. RESULTS AND DISCUSSION

The aim of this work consists in finding a theoretical model able to reproduce the recent experimental results published by Milne-Brownlie [35] concerning the relative TDCS's for the ionization of the four outer orbitals of the water molecule $^1B_1$, $^3A_1$, $^1B_2$, and $^2A_1$ whose experimental binding energies are 12.6, 14.7, 18.5, and 32.2 eV, respectively. The experimental conditions are the following: the incident energy $E_i = 250$ eV and the ejected energy $E_e = 10$ eV (except for the $^3A_1$ molecular orbital for which the ejected electron has an energy of $E_e = 8$ eV) while the geometrical conditions are given by: $\varphi_s = 180°$, $\varphi_e = 0°$, and $\theta_s = 15°$. Moreover, it is also important to note that the TDCS's presented in this work are obtained by analytical integration of more differential cross sections (denoted in the following 4DCS's) which correspond to the ionization cross sections of a fixed water molecule whose orientation is defined by means of the Euler angles (α,β,γ) (see [36] for more details). The 4DCS is defined by

$$\sigma^{(4)} = \frac{d^4\sigma}{d\Omega_{Euler}d\Omega_e d\Omega_s dE_e}, \tag{25}$$

where $d\Omega_{Euler} = \sin\beta\, d\beta\, d\alpha\, d\gamma$. Considering the description proposed by Moccia corresponding to a given molecular ori-

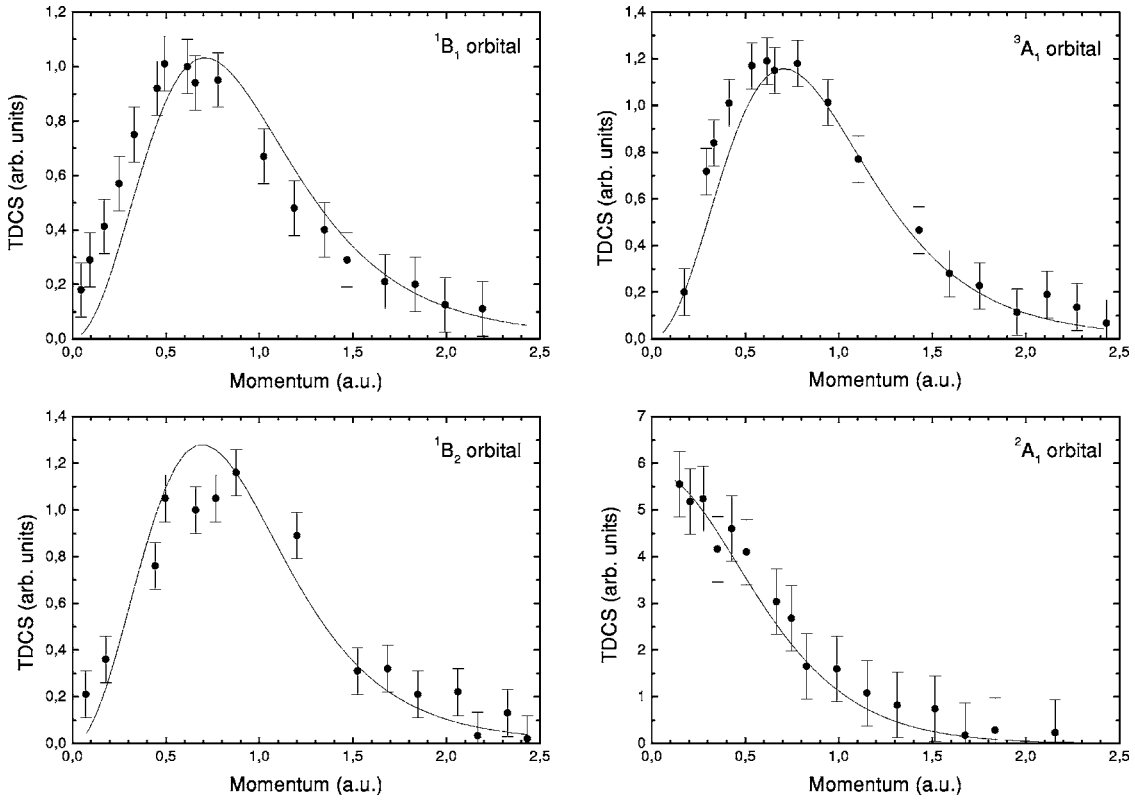

FIG. 1. Comparison between the present theoretical results (solid line) and the experimental momentum profiles (solid circles) for a noncoplanar symmetric geometry where the outgoing electrons are detected at $\theta=45°$ sharing the same energy $E=600$ eV (Bawagan *et al.* [52]).

entation in the space [39], we have to average the 4DCS's over the Euler solid angle $d\Omega_{Euler}$ to obtain TDCS's comparable to the experimental results. In fact, this "space integration" is analytically carried out, even for the very sophisticated and very time consuming models such as BBK and DS3C, thanks to the following property for the rotation matrix:

$$\frac{1}{8\pi^2}\int d\Omega_{Euler} D^{l}_{\mu,m}(\alpha,\beta,\gamma) D^{l'^{*}}_{\mu',m'}(\alpha,\beta,\gamma) = \frac{1}{\hat{l}}\delta_{l,l'}\delta_{m,m'}\delta_{\mu,\mu'}, \tag{26}$$

where $\hat{l}=2l+1$.

In all cases the relative measurements under investigation will be normalized to our theoretical calculations so as to give the best visual fit.

A. EMS (electron momentum spectroscopy) comparison

First of all, let us start the present subsection by discussing the accuracy of the molecular wave functions proposed by Moccia for describing simple molecular targets such as H_2O as well as NH_3 and CH_4 by means of single-center expansion of Slater-like functions. To do that we have compared the theoretical TDCS's obtained by using the wave functions of Moccia [39] to the electron momentum spectroscopy experimental results published by Bawagan *et al.* [52]. Indeed, the EMS technique, formerly known as binary $(e,2e)$ spectroscopy, constitutes a powerful tool for studying the atomic and molecular orbitals [1,2]. In fact, in these experiments, the measured TDCS's are directly related to the square of the spherically averaged electron momentum distribution ($|\Psi(\vec{p})|^2$) at any selected binding energy which can be obtained by means of Fourier transforms of the familiar position space wave function $\Psi(\vec{r})$. The experiments are generally performed at intermediate energies (about 1–2 keV) in a noncoplanar geometry with two outgoing electrons sharing the energy evenly and detected at equal θ polar angles with respect to the incident electron direction. The TDCS's thus obtained are usually plotted versus the recoil momentum q defined by

$$q = \left[[2k_e\cos(\theta) - k_i]^2 + 4k_e^2\sin^2(\theta)\sin^2\left(\frac{\Phi}{2}\right)\right]^{1/2}, \tag{27}$$

where θ is the polar angle and Φ is given by $\Phi=\pi-|\varphi_s-\varphi_e|$; $(\varphi_s-\varphi_e)$ is defined as the relative azimuthal angle between the two outgoing electrons. The geometrical conditions of the present TDCS measurements are φ_s ranging from 0° to 30°, $\varphi_e=0°$, and θ constant. The momentum transfer to the target is rather large (4–7 a.u.) and the process is simple enough to be investigated by first order theories. Within this geometry, our theoretical results based on the plane wave impulse approximation (PWBA) can be compared to the EMS experiments without forgetting to take into account the exchange effects, since the two outgoing electrons have the

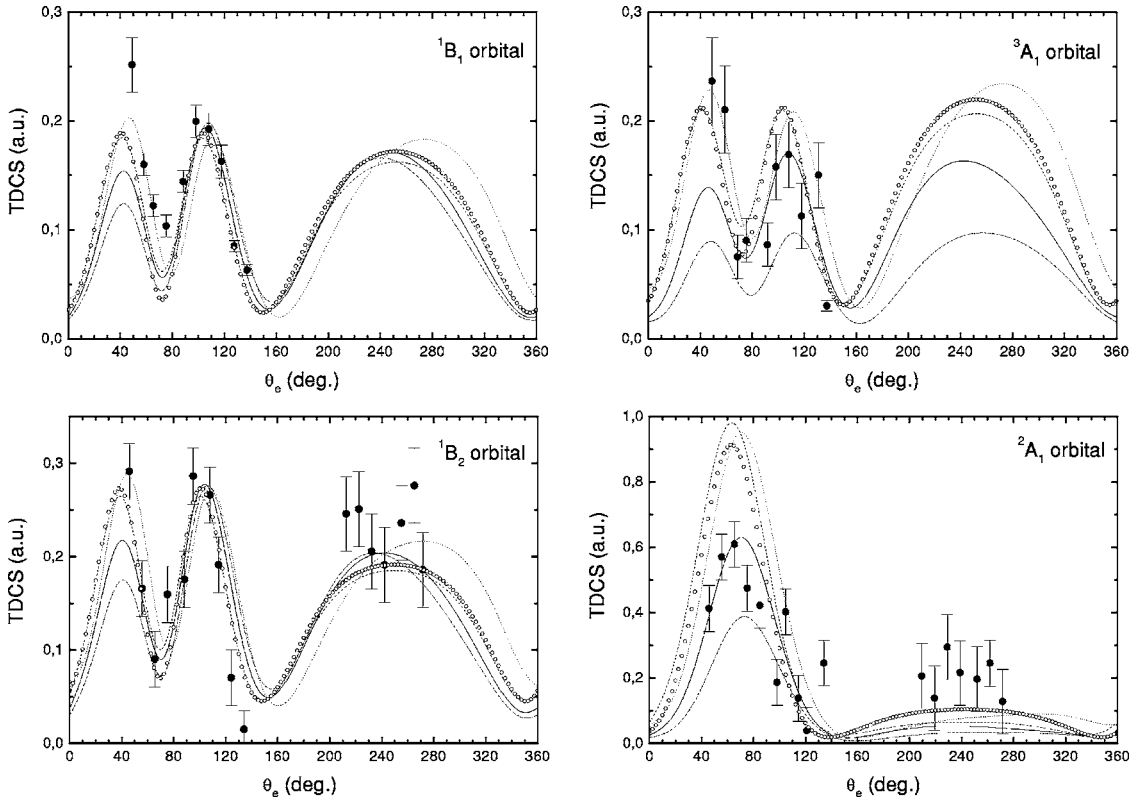

FIG. 2. TDCS's for electron-impact ionization of the four outer molecular orbitals of H_2O. Comparison between the experimental data (solid circles) of Milne-Brownlie *et al.* [35] and the theoretical results obtained in the different models investigated in the present work: (i) the 1CW model (dashed line), (ii) the DWBA model (open circles), (iii) the 2CW model (dotted line), (iv) the BBK model (dash-and-dotted line), and (v) the DS3C (solid line) model.

same energy in the final state. The experiments under investigation are those of Bawagan *et al.* [52] performed with impact energy of about 1200 eV, a detection angle of $\theta = 45°$ corresponding to the maximum momentum transfer of 6.6 a.u. Figure 1 shows the results we have obtained for the ionization of the $^1B_1$, $^3A_1$, $^1B_2$, and $^2A_1$ orbitals, respectively. The good agreement observed indicates that the initial wave function describing the target is of good quality and constitutes *an accurate description of the target structure*. On the other hand, the molecular energy and the electric dipole moment computed by using this wave function are very close to the experimental values (see [39] for experimental and/or theoretical comparisons of the geometrical properties of the water molecule). Likewise it is important to note that this wave function, developed on a basis of Slater-like functions, reproduces quasi-similar results to those developed on a basis of Gaussian-like functions but with more than 100 terms in the expansion [52].

B. TDCS calculations

Let us now consider the recent measurements of TDCS's performed in an asymmetric coplanar geometry at low incident energy [35]. As detailed above, the experiment has been performed at incident and ejected electron energies of 250 and 10 eV (except for the $^3A_1$ orbital for which the ejected electron has an energy of 8 eV), respectively, while the scattered electron is detected at 15° with respect to the incident beam. In all cases, the theoretical results are performed with the analytical formulas given in Eq. (17) [42], and have been successfully compared to the results obtained in the partial wave technique [37] in the 1CW model. Let us note also that, in contrast to the EMS treatment, the exchange effects are here omitted since the scattered electron is faster than the ejected one in all the experiments considered.

In Fig. 2, the present TDCS calculations for electron-impact ionization of the four outer molecular orbitals of H_2O performed in the five models described above are compared to the experimental data of Milne-Brownlie *et al.* [35]. We observe that the 1CW and the DWBA models (dashed line and open circles, respectively), which represent a first order approach are able to produce a considerable improvement by comparison to the results presented in [35] (where contribution of the nucleus in the interaction was neglected). Indeed, a recoil peak is now observed in the two approaches. However, the two models are not able to reproduce the experimental measurements in the small-ejected angle region, i.e., the first structure of the binary region. For the four considered molecular orbitals, the DWBA model tends to increase the recoil peak and decrease the binary peak compared to the results obtained in the 1CW model. We note that the recoil peak for the $^2A_1$ orbital is not correctly reproduced by the two models since the theory underestimates the experiments. Furthermore, the 2CW model (dotted line) seems to show a little bit better agreement with the experiments than the 1CW

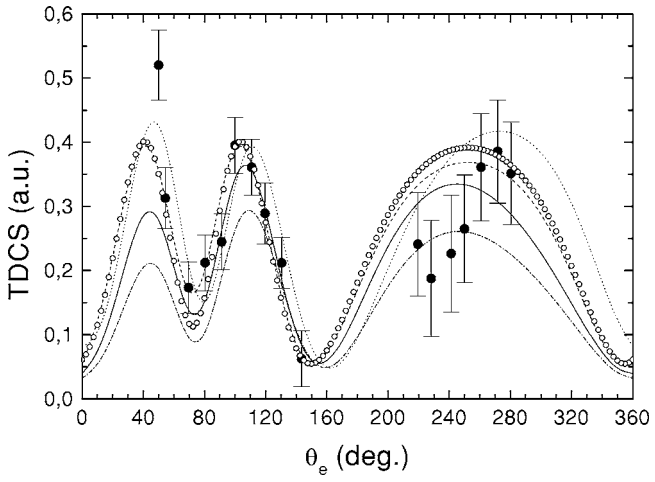

FIG. 3. Summed TDCS's for electron-impact ionization of the $^1B_1$ and $^3A_1$ orbitals of H_2O. The theoretical calculations are performed in (i) the 1CW model (dashed line), (ii) the DWBA model (open circles), (iii) the 2CW model (dotted line), (iv) the BBK model (dash-and-dotted line), and (v) the DS3C (solid line) model. The experimental data (solid circles) are taken from [35].

model. Indeed, the 2CW peaks of the binary and the recoil regions are slightly shifted towards larger angles with respect to those obtained in the 1CW model. The magnitudes are also enhanced in the 2CW approach except in the binary peak of the $^2A_1$ orbital. The small discrepancies observed between these two models (1CW and 2CW) can be explained by the fact that the (fast) scattered electron (whose energy is high compared to the ejected one) interacts weakly with the target nucleus and can therefore, in this particular case, be described either by a Coulomb wave or by a plane wave.

Considering the two other more sophisticated models (BBK and DS3C), we observe that the experiments are well reproduced, except for lower angles in the binary region where the experimental data are underestimated. We notice that the DS3C results are closer to the experiments than those obtained in the BBK model. Moreover, comparisons of all the different models studied here show that the results obtained for the $^2A_1$ orbital in the BBK and DS3C models are in better agreement with the experiment.

In Fig. 3, the TDCS's of the $^1B_1$ and $^3A_1$ orbitals are summed and compared to the experimental data. The five approaches are able to reproduce the recoil peak in contrast with the rather simplified model based on the DWBA treatment previously used in [35]. Nevertheless, none of these models is able to correctly describe the entire binary region as already pointed out in [18] where similar results were found for the ionization of H_2 and He by electron impact.

IV. CONCLUSION

On the basis of the present calculations, we can first conclude that our models correctly reproduce the recoil peaks observed in most of the cases investigated in this work. Generally speaking, the two first order models (1CW and DWBA) reproduce quite well the shape of the TDCS's except for the $^2A_1$ orbital where the recoil peak is underestimated. The 2CW model gives better agreement with experiments than the first cited ones, the recoil peak remaining still underestimated in the case of $^2A_1$ orbital. When the more sophisticated BBK and DS3C models are investigated, a good agreement with experiments is observed too. For all models, the double structure of the binary region is generally well reproduced as in the case of the rather simplified DWBA approach [35]. However, none of the models (even the rather sophisticated DS3C approach) reproduces correctly the data at lower ejection angles.

Moreover, it is also important to notice that thanks to the analytical aspect of the integration method over the molecular orientation, it is now possible to provide more easily integrated cross sections like double, single, and total cross sections. Work in this aspect is currently in progress for H_2O and other small molecules such as CH_4, NH_3, whose interest has recently grown in view of their important role in the development of technological plasma devices, and even in radiobiology where they are commonly used to simulate the organic matter.

ACKNOWLEDGMENT

We are very grateful to Professor A. C. Roy for many fruitful discussions and comments about this work. Partial financial support for this work was provided by PROJET CMEP 05 MDU 650. The authors would like to thank the CINES (Centre Informatique National de l'Enseignement Superieur) of Montpellier (France) for free computer time.

APPENDIX

The calculation of the matrix element in Eq. (12) with the formula given in Eq. (19) needs the following basic integral [17]:

$$
\begin{aligned}
&J(\lambda,c,a,\vec{u},\vec{\nu},\vec{w},\vec{k}_s,\vec{k}_e,\vec{p}) \\
&\quad=\int d\vec{r}_0 d\vec{r}_1 \frac{\exp(-\lambda r_{01})}{r_0 r_1 r_{01}} \exp(-cr_0)\exp(-ar_1) \\
&\qquad\times\exp(i(\vec{u}-\vec{k}_s+\vec{p})\vec{r}_0)\exp(i(\vec{\nu}-\vec{k}_e+\vec{w})\vec{r}_1) \\
&\qquad\times{}_1F_1\left[iZ_e/k_e,1,i(\vec{k}_e\vec{r}_1+\vec{k}_e r_1)\right] \\
&\qquad\times{}_1F_1\left[iZ_s/k_s,1,i(\vec{k}_s\vec{r}_0+\vec{k}_s r_0)\right] \\
&\qquad\times{}_1F_1\left[-iZ_{se}/k_{se},1,i(\vec{k}_{se}\vec{r}_{01}+\vec{k}_{se} r_{01})\right].
\end{aligned}
$$

This six-dimensional integral can be reduced to a two-dimensional integral by using the well-known method of Roy *et al.* [53] and that of Brauner *et al.* [17]. In this problem we have to work with $1s, 2s, 3d$, and $4f$ orbitals which needs, respectively, two, three, four, and five derivations of $J(\lambda,c,a,\vec{u},\vec{\nu},\vec{w},\vec{k}_s,\vec{k}_e,\vec{p})$. Our work follows those of Hafid *et al.* [54] (for $2s$ and $2p$ orbitals) and of Cheikh *et al.* [55] (for $3s, 3p$, and $3d$).

For instance, for the case of $4f_0$ [where $Y_3^0=-\sqrt{7}(3\cos\theta-5\cos^3\theta)/4\sqrt{\pi}$], the matrix element given in Eq. (12) needs the following terms:

$$M \sim \frac{1}{2\pi}\left\{ 5i\left(\frac{7}{16\pi}\right)^{1/2} \frac{\partial^5}{\partial c\, \partial a\, \partial w_z^3} \times J(\lambda=0,c,a,\vec{k}_i,\vec{\nu}=\vec{0},\vec{w}=\vec{0},\vec{k}_s,\vec{k}_e,\vec{p}=\vec{0}) + \frac{1}{2}i\left(\frac{63}{4\pi}\right)^{1/2} \times \frac{\partial^5}{\partial c\, \partial a^3\, \partial w_z} J(\lambda=0,c,a,\vec{k}_i,\vec{\nu}=\vec{0},\vec{w}=\vec{0},\vec{k}_s,\vec{k}_e,\vec{p}=\vec{0}) - 5i\left(\frac{7}{16\pi}\right)^{1/2} \frac{\partial^5}{\partial\lambda\, \partial a\, \partial w_z^3} J(\lambda=0,c,a,\vec{k}_i,\vec{\nu}=\vec{0},\vec{w}=\vec{0},\vec{k}_s,\vec{k}_e,\vec{p}=\vec{0}) - \frac{1}{2}i\left(\frac{63}{4\pi}\right)^{1/2} \frac{\partial^5}{\partial\lambda\, \partial a^3\, \partial w_z} \times J(\lambda=0,c,a,\vec{k}_i,\vec{\nu}=\vec{0},\vec{w}=\vec{0},\vec{k}_s,\vec{k}_e,\vec{p}=\vec{0}) \right\}.$$

Each term has been carefully checked with the analytic formulas of Dal Cappello *et al.* [42] when $Z_s=0$ and $Z_{se}=0$. When only $Z_{se}=0$, we obtain a matrix element similar to that obtained in the 2CW model (one numerical integration in this case).

[1] M. Coplan, J. H. Moore, and J. P. Doering, Rev. Mod. Phys. **66**, 985 (1994).
[2] A. Lahmam-Bennani, J. Phys. B **24**, 2401 (1991).
[3] K. Jung, E. Schubert, P. A. L. Paul, and H. Ehrhardt, J. Phys. B **8**, 1330 (1975).
[4] M. Cherid, A. Lahmam-Bennani, A. Duguet, R. R. Zurales, R. W. Lucchese, M. C. Dal Cappello, and C. Dal Cappello, J. Phys. B **22**, 3483 (1989).
[5] L. Avaldi, R. Camilloni, E. Fainelli, and G. Stefani, J. Phys. B **25**, 3551 (1992).
[6] J. P. Doering and J. Yang, Phys. Rev. A **54**, 3977 (1996).
[7] S. Rioual, V. Nguyen, and A. Pochat, Phys. Rev. A **54**, 4968 (1996).
[8] S. J. Cavanagh and B. Lohmann, J. Phys. B **32**, L261 (1999).
[9] J. Yang and J. P. Doering, Phys. Rev. A **63**, 032717 (2001).
[10] S. M. Younger and T. D. Märk, in *Electron Impact Ionization*, edited by T. D. Märk and G. H. Dunn (Springer, Berlin, 1985), Chap. 2.
[11] S. P. Khare and W. J. Meath, J. Phys. B **20**, 2101 (1987).
[12] Y-K. Kim and M. E. Rudd, Phys. Rev. A **50**, 3954 (1994).
[13] Y-K. Kim and M. E. Rudd, Comments At. Mol. Phys. **34**, 293 (1999).
[14] L. Vriens, in *Case Studies in Atomic Physics*, edited by E. W. McDaniel and M. R. C. McDowell (North-Holland, Amsterdam, 1969), Vol. 1, p. 335.
[15] H. Bethe, Ann. Phys. **5**, 325 (1930).
[16] R. W. Zurales and R. R. Lucchese, Phys. Rev. A **37**, 1176 (1988).
[17] M. Brauner, J. S. Briggs, and H. Klar, J. Phys. B **22**, 2265 (1989).
[18] S. Houamer, A. Mansouri, C. Dal Cappello, A. Lahmam-Bennani, S. Elazzouzi, M. Moulay, and I. Charpentier, J. Phys. B **36**, 3009 (2003).
[19] C. Stia, O. Fojon, P. Weck, J. Hanssen, B. Joulakian, and R. D. Rivarola, Phys. Rev. A **66**, 052709 (2002).
[20] C. B. Opal, E. C. Beaty, and W. K. Peterson, At. Data **4**, 209 (1972).
[21] M. A. Bolorizadeh and M. E. Rudd, Phys. Rev. A **33**, 882 (1985).
[22] N. Oda, Radiat. Res. **64**, 80 (1975).
[23] N. Lj. Djuric, I. M. Cadez, and M. V. Kurepa, Int. J. Mass Spectrom. Ion Process. **83**, R7 (1988).
[24] J. Schutten, F. J. de Heer, H. R. Moustafa, A. J. H. Boerboom, and J. Kistenmaker, J. Chem. Phys. **44**, 3924 (1966).
[25] M. V. V. Rao, I. Iga, and S. K. Srivastava, J. Geophys. Res. **100**, 26421 (1995).
[26] S. P. Khare and W. J. Meath, J. Phys. B **20**, 2101 (1987).
[27] H. C. Straub, B. G. Lindsay, K. A. Smith, and R. F. Stebbings, J. Chem. Phys. **108**, 109 (1998).
[28] T. J. Dolan, J. Phys. D **26**, 4 (1993).
[29] K. W. Hollman, G. W., Kerby III, M. E. Rudd, J. H. Miller, and S. T. Manson, Phys. Rev. A **38**, 3299 (1988).
[30] D. A. Vroom and R. L. Palmer, J. Chem. Phys. **66**, 3720 (1977).
[31] J. J. Olivero, R. W. Stagat, and A. E. S. Green, J. Geophys. Res. **77**, 4797 (1972).
[32] J. C. Gomet, C. R. Acad. C. R. Seances Acad. Sci., Ser. B **B281**, 627 (1975).
[33] T. D. Märk and F. Egger, Int. J. Mass Spectrom. Ion Phys. **20**, 89 (1976).
[34] O. J. Orient and S. K. Srivastava, J. Phys. B **20**, 3923 (1987).
[35] D. S. Milne-Brownlie, S. J. Cavanagh, B. Lohmann, C. Champion, P.-A. Hervieux, and J. Hanssen, Phys. Rev. A **69**, 032701 (2004).
[36] C. Champion, J. Hanssen, and P.-A. Hervieux, Phys. Rev. A **63**, 052720 (2001).
[37] C. Champion, J. Hanssen, and P.-A. Hervieux, Phys. Rev. A **65**, 022710 (2002).
[38] A. L. Monzani, L. E. Machado, and M.-Td. A. M. Machado, Phys. Rev. A **60**, R21 (1999).
[39] R. Moccia, J. Chem. Phys. **40**, 2186 (1964).
[40] C. Champion, J. Hanssen, and P.-A. Hervieux, Phys. Rev. A **72**, 059906(E) (2005).
[41] H. Trygve, P. Jorgensen, and J. Olsen, *Molecular Electronic-Structure Theory* (John Wiley Sons, New York, 2000).
[42] C. Dal Cappello, C. Tavard, A. Lahmam-Bennani, and M. C. Dal Cappello, J. Phys. B **17**, 4557 (1984).
[43] M. J. Brothers and R. A. Bonham, J. Phys. B **17**, 4235 (1984).
[44] M. Schulz, J. Phys. B **6**, 2580 (1973).
[45] A. J. Murray and F. H. Read, J. Phys. B **26**, L359 (1993).
[46] T. Rösel, J. Röder, L. Frost, K. Jung, H. Ehrhardt, S. Jones, and D. H. Madison, Phys. Rev. A **46**, 2539 (1992).
[47] M. Brauner, J. S. Briggs, H. Klar, J. T. Broad, T. Rösel, K. Jung, and H. Ehrhardt, J. Phys. B **24**, 657 (1991).
[48] J. Berakdar and J. S. Briggs, Phys. Rev. Lett. **72**, 3799 (1994).
[49] S. Zhang, J. Phys. B **33**, 3545 (2000).
[50] J. Röder, H. Ehrhardt, I. Bray, D. V. Fursa, and I. E. McCarthy, J. Phys. B **29**, L67 (1996).

[51] D. V. Fursa and I. Bray, Phys. Rev. A **52**, 1279 (1995).
[52] A. O. Bawagan, C. E. Brion, E. R. Davidson, and D. Feller, J. Chem. Phys. **113**, 19 (1987).
[53] A. Roy, K. Roy and N. C. Sil, J. Phys. B **13**, 3443 (1980).
[54] H. Hafid, B. Joulakian, and C. Dal Cappello, J. Phys. B **26**, 3415 (1993).
[55] R. Cheikh, J. Hanssen, and B. Joulakian, Eur. Phys. J. D **2**, 203 (1998).